

UC Davis

UC Davis Previously Published Works

Title

Circulating immunity protects the female reproductive tract from Chlamydia infection

Permalink

<https://escholarship.org/uc/item/3b6457zw>

Journal

Proceedings of the National Academy of Sciences of the United States of America,
118(21)

ISSN

0027-8424

Authors

Labuda, Jasmine C
Pham, Oanh H
Depew, Claire E
et al.

Publication Date

2021-05-25

DOI

10.1073/pnas.2104407118

Peer reviewed



Circulating immunity protects the female reproductive tract from *Chlamydia* infection

Jasmine C. Labuda^a, Oanh H. Pham^a, Claire E. Depew^a, Kevin D. Fong^a, Bokyoung Lee^{a,1}, Jordan A. Rixon^a, and Stephen J. McSorley^{a,2}

^aCenter for Immunology and Infectious Diseases, Department of Anatomy, Physiology, and Cell Biology, School of Veterinary Medicine, University of California, Davis, CA 95616

Edited by Yasmine Belkaid, NIH, Bethesda, MD, and approved April 3, 2021 (received for review March 8, 2021)

Anatomical positioning of memory lymphocytes within barrier tissues accelerates secondary immune responses and is thought to be essential for protection at mucosal surfaces. However, it remains unclear whether resident memory in the female reproductive tract (FRT) is required for Chlamydial immunity. Here, we describe efficient generation of tissue-resident memory CD4 T cells and memory lymphocyte clusters within the FRT after vaginal infection with *Chlamydia*. Despite robust establishment of localized memory lymphocytes within the FRT, naïve mice surgically joined to immune mice, or mice with only circulating immunity following intranasal immunization, were fully capable of resisting *Chlamydia* infection via the vaginal route. Blocking the rapid mobilization of circulating memory CD4 T cells to the FRT inhibited this protective response. These data demonstrate that secondary protection in the FRT can occur in the complete absence of tissue-resident immune cells. The ability to confer robust protection to barrier tissues via circulating immune memory provides an unexpected opportunity for vaccine development against infections of the FRT.

female reproductive tract | CD4 T cells | *Chlamydia*

Naïve CD4 T cells circulate through lymphoid tissues and blood until an infection initiates lymphocyte clonal expansion and the acquisition of specific effector function (1, 2). Expanded effector CD4 T cells access inflamed or infected tissues where they regulate pathogen control and coordinate tissue repair (3, 4). In the aftermath of this host response, an elevated frequency of memory CD4 T cells returns to circulation, and a discrete population of noncirculating memory lymphocytes is retained within the tissues (5, 6). For many barrier tissues, the noncirculating tissue-resident memory T cells (T_{RM}) are critical for the rapid deployment of secondary immune responses upon pathogen reexposure (6–11). The female reproductive tract (FRT) is a barrier tissue that is thought to depend heavily on T_{RM} since it regularly encounters pathogens but lacks organized lymphoid tissues (12).

The lack of organized lymphoid structures during steady-state and the immunologically restrictive nature of the FRT makes establishing immunity in this mucosal tissue a complex process. In certain contexts, lymphocytes as well as circulating antibody cannot easily enter the FRT mucosa (9, 10), suggesting that protective immune memory is contained within the tissue itself. Indeed, previous reports document the establishment of resident memory lymphocytes and mucosal antibody secretion as two important local protective mechanisms (7, 9, 13). Memory lymphocyte clusters (MLCs) are lymphoid structures that form at the interface of the FRT epithelium and lamina propria and consist of memory T cells and antigen presenting cells (13). Upon secondary infection, these MLCs can efficiently recruit effector cells in a CD4 T cell–dependent manner to clear FRT infections (9, 13). Thus, the generation of FRT MLCs is thought to be an important prerequisite for the development of new vaccines against important reproductive tract pathogens.

A confusing aspect of this model is the observation that distal mucosal immunization in the lung can often induce local

immunity in the FRT. It is not yet clear whether such distal immunization induces seeding the FRT with T_{RM} , formation of MLCs, and/or secretion of local antibody (14, 15). An alternative hypothesis is that distal immunization generates circulating memory responses that are recruited to the infected FRT and mediate pathogen clearance in the absence of T_{RM} or MLCs (15, 16).

In this study, we examined whether local or distal immunization with the bacterial pathogen *Chlamydia muridarum* (*Cm*) is protective against intravaginal (I.Vag) challenge with *Chlamydia*. Our data reveal that CD4 T_{RM} efficiently populate the FRT and that MLCs are generated after local, but not distal, immunization. Using parabiosis, we demonstrate that the establishment of local resident memory lymphocytes in the FRT is dispensable for protective immunity. Indeed, circulating immunity induced locally or distally was completely sufficient for protection against local infection and FRT pathology. The depletion of lymphocytes revealed that local control of protection was mediated by circulating memory CD4 T cells.

Methods

Mice. C57BL/6 mice were purchased from The Jackson Laboratory at 8 to 16 wk of age and housed under specific pathogen-free conditions. All animal

Significance

Sexually transmitted infections are widespread and cause irreparable harm to young women. After infection of the female reproductive tract, lymphoid clusters are generated with fully resident lymphocytes that do not recirculate via blood or lymphatic vessels. However, the protective value of tissue-resident lymphocytes or cluster formation has not been determined for important reproductive pathogens. Our study demonstrates that these local immune structures are unnecessary for robust protective immunity to *Chlamydia*. Instead, efficient tissue surveillance is provided by circulating memory lymphocytes generated outside reproductive tissues. These findings reinforce the value of assessing circulating, rather than local, immune parameters of *Chlamydia* immunity and suggest that future vaccine efforts should focus on the elicitation of robust systemic immunity to provide local mucosal protection.

Author contributions: J.C.L. and S.J.M. designed research; J.C.L., O.H.P., C.E.D., K.D.F., B.L., and J.A.R. performed research; J.C.L. and S.J.M. analyzed data; and J.C.L. and S.J.M. wrote the paper.

The authors declare no competing interest.

This article is a PNAS Direct Submission.

Published under the PNAS license.

¹Present address: Department of Food Science and Nutrition, College of Health Sciences, Dong-A University, Busan 602760, South Korea.

²To whom correspondence may be addressed. Email: sjmcsorley@ucdavis.edu.

This article contains supporting information online at <https://www.pnas.org/lookup/suppl/doi:10.1073/pnas.2104407118/-DCSupplemental>.

Published May 17, 2021.

experiments were approved by the Institutional Animal Care and Use Committee at University of California (UC) Davis.

Bacterial Infection. Mice were synchronized by subcutaneous injection of 2.5 mg Depo provera 7 d prior to I.Vag infection. *Cm* was purchased from American Type Culture Collection and propagated using established culture conditions (5, 6). For I.Vag infections, 10^5 inclusion forming units (IFU) of *Cm* was suspended in 5 μ L SPG buffer and pipetted into the vagina. For intranasal (IN) infection, 10^5 IFU of *Cm* (in 20 μ L SPG buffer) was pipetted into the nasal cavity of anesthetized mice.

Enumeration of Bacteria. *Chlamydia* bacterial burden was measured by cervico-vaginal swabbing and culture. Vaginal swabs were placed in 500 μ L SPG buffer with glass beads and disrupted for 5 min. Serial dilutions were generated from swab supernatants and subsequently plated on HeLa229 monolayers. Infected cells were fixed with methanol and stained using a primary mouse anti-*Chlamydia* Major Outer Membrane Protein antibody that was a kind gift from the Caldwell laboratory. Antibody-stained HeLa cells were further incubated with a goat, anti-mouse, fluorescein isothiocyanate (FITC)-conjugated IgG secondary antibody and IFU enumerated using a Keyence microscope.

ELISPOT Assays. Enzyme-linked immune absorbent spot (ELISPOT) plates were prepared using the Mouse Interferon Gamma ELISPOT Kit from BD, following the manufacturer's protocol. Single cell suspensions were prepared from tissues and labeled for negative selection with Miltenyi Biotec CD4 selection kits. Cells from the FRT underwent a second round of positive CD4 selection to remove epithelial cell contamination. CD4 T cells were routinely isolated to 80 to 90% purity using this approach. After column enrichment, 10^5 splenocyte cells or all the recovered FRT cells (10^5 or less) were plated into precoated ELISPOT plates and incubated overnight with medium, heat-killed elementary bodies (HKEBs), heat-killed *Salmonella typhimurium*, or anti-CD3/CD28 (5 μ g/mL and 1 μ g/mL). Plates were subsequently washed with 0.5% PBS-Tween and stained with detection antibody and a horseradish peroxidase (HRP)-conjugated antibody. After the final wash, AEC substrate was added to wells and spots counted using an AID ELISPOT Reader (Autoimmune Diagnostika).

ELISAs. 5×10^5 IFU of heat-killed *Cm* was coated onto a 96-well enzyme-linked immunosorbent assay (ELISA) plate (Corning Costar) with PBS and incubated overnight at 4 °C. Serum was diluted 1:10,000 for the IgG ELISA, and 1:10 for IgA ELISA. Vaginal lavage (VL) samples were diluted 1:10. All samples were serially diluted 1:2. Plates were washed three times with 0.05% PBS-Tween20 (PBST), and then 0.5% bovine serum albumin (BSA) was incubated on the plate for 1 h at room temperature (RT) to block nonspecific binding. Diluted serum or VL samples were added to plates after blocking and incubated for 2.5 h at RT. Plates were then washed four times with PBST, and anti-mouse IgA-biotin (eBioscience) or anti-mouse IgG-biotin (eBioscience) diluted 1:500 was added to plates and incubated for 1 h at RT. Plates were washed four times with PBST and then incubated with avidin-HRP (eBioscience Ready-Set-Go) for 30 min at RT. Plates were washed again, and then 3,3',5,5'-tetramethylbenzidine (TMB) substrate was added for 15 min and stopped with sulfuric acid.

Serum Transfers. *Cm*-immune or naïve mice were bled, and serum was collected. For passive immune serum transfer, mice were injected intraperitoneal (i.p.) with 200 μ L serum diluted up to 500 μ L in PBS every 3 d. For I.Vag serum transfers, mice were given 20 μ L immune serum or naïve serum pipetted directly into the vaginal vault.

Flow Cytometry. Intravascular lymphocyte staining was performed by injecting 3 μ g/ μ L antibody specific for CD45 or CD90 into the tail vein of mice 3 min prior to euthanasia. Single cell suspensions were blocked using 24G2 antibody 10 to 30 min prior to antibody staining. Antibodies used in this study include APC: CD11b, CD11c, F4/80, B220 CD44, and CD4; FITC: CD62L, CD11b, CD11c, F4/80, B220, CD69, and CD4; AF700: CD4 and CD44; PEcy7: CD44; PerCP EF710: CD90.2 and CD8; BV650: CD45.1 and CD45.2; EF450: CD69 and CD3; PE Texas Red CD62L; PE: P2RX7, CD11b, CD11c, F4/80, and B220; and APC EF780: CD11b, CD11c, F4/80, and B220. Samples were analyzed on a BD LSR Fortessa or FACS Symphony, and results were analyzed using FlowJo software.

Lymphocyte Isolation. Spleens were processed as previously described (6). FRTs were initially diced into small tissue pieces before being digested in 25-mL

flasks containing collagenase IV in 5% RPMI medium. FRTs were disrupted for 1 h and then strained carefully to remove any larger tissue clumps. FRT lymphocytes were subsequently isolated from these suspensions using 44 and 67% Percoll gradients.

Parabiosis. Mouse parabiosis was performed, as previously described (6). Briefly, CD45.1 mice were infected with *Cm* intravaginally and allowed to completely resolve the primary infection and develop memory responses for ~2 mo. These CD45.1-immune mice were then surgically joined to CD45.2-naïve mice and monitored carefully to ensure successful surgery and wound healing. Similarly, naïve mice were surgically joined to other naïve mice and referred to as "surgery controls." The blood of all cojoined mice was assessed after 12 to 14 d of parabiosis to confirm that blood chimerism had occurred. Following successful parabiosis, surgery was reversed, and separated mice were rested for 2 wk before further experimentation. Parabionts (both naïve and memory) were infected intravaginally with *Chlamydia* and bacterial shedding was examined, as described above. In all protection experiments, groups of naïve and immune mice that had not undergone surgery were also infected as controls.

Histology. The entire reproductive tract was harvested from female mice and frozen in optimal cutting temperature (OCT) on dry ice. Tissue blocks were sectioned on a Leica CM3050S cryostat at 10- μ m thickness and sampled at 50- μ m intervals throughout the tissue. Slides were fixed in ice-cold acetone and frozen at -80 °C until stained. For staining, slides were thawed and rehydrated in PBS before 5% BSA was used to block for 30 min. Slides were subsequently stained with anti-mouse CD4 PE/Dazzle (clone RM4-5, Biogen) for 2 h before being washed in PBS and counterstained with DAPI. Slides were imaged using a Leica SP8 stimulated emission depletion (STED) 3X microscope using stitching of 1,248 μ m \times 1,248 μ m images to achieve an image of the entire reproductive tract section. To enumerate clusters in reproductive tract tissues, ImageJ software was first used to mask and calculate the area of DAPI staining for each tissue section. Another investigator, blinded to treatment groups, counted the number of CD4+ clusters with a minimum radius of 75 μ m in each tissue section. The area of DAPI for each tissue section was extracted, and the cluster number per tissue was divided by the DAPI area of each tissue. This method was used to account for variation in the area of tissue sections.

Histopathological Analysis. Naïve or infected mice were sacrificed at 30 d postsecondary infection by carbon dioxide asphyxiation and cardiac exsanguination. The FRT (ovary, oviduct, uterus, cervix, and vagina) was immersed fixed in 10% neutral buffered formalin. Fixed tissues were embedded in paraffin, sectioned 5- μ m thick, and stained with hematoxylin and eosin. Histopathologic evaluation was performed by a board-certified veterinary anatomic pathologist after masking and randomization of samples. Samples were evaluated for the presence and severity of acute inflammation, chronic inflammation, erosion, dilation, and fibrosis. Acute inflammation was defined by neutrophilic infiltration and edema. Chronic inflammation was defined by lymphohistiocytic infiltration. Erosion was defined by the loss of mucosal epithelial cells, with or without breach of the basement membrane. Dilation was defined by distention of the lumen. Fibrosis was defined by either an increase in fibroblasts or an increase in collagenous connective tissue. Parameters were evaluated using an ordinal scoring system based on lesion severity and distribution on a 0- to 4-point scale.

Lymphocyte Depletion. A total of 300 μ g Anti-CD4 clone GK1.5 and Isotype control antibody clone LTF2 antibodies (Bio X Cell) were administered to mice i.p. every 3 to 4 d beginning 4 d prior to secondary infection and ending 18 d postinfection.

Statistics. Statistical analysis was performed by using an unpaired *t* test for normally distributed continuous variable comparisons and a Mann-Whitney *U* test for nonparametric comparisons (Prism; GraphPad Software, Inc.). Graphical figures were made using Biorender (<https://biorender.com/>).

Results

***Chlamydia*-Specific CD4 T_{RM} Populate the FRT after Local Infection with *Chlamydia*.** To determine whether CD4 T_{RM} are generated after I.Vag exposure to *Cm*, C57BL/6 mice were infected with 10^5 IFU *Cm* and reproductive tract tissues examined 65 d later. There was an obvious increase in the percentage of antigen-experienced effector CD4 T cells (CD44^{hi} CD62L⁻) in the reproductive tract, and most of these cells expressed phenotypic

markers of tissue-resident memory (CD69⁺ P2RX7⁺) (Fig. 1 *A* and *B*). The absolute number of CD4 T cells in the FRT increased markedly after *Chlamydia* infection, and much of this increase was due to an increase in resident memory cells (Fig. 1*B*). IFN- γ ELISPOT analysis confirmed that CD4 T cells in the FRT and spleen were reactive to *Chlamydia* HKEBs (Fig. 1 *C* and *D*). Thus, *Chlamydia*-specific CD4 T_{RM} populate the FRT of C57BL/6 mice after the resolution of I.Vag *Cm* infection.

Circulating Immunity Is Sufficient for Secondary Protection against *Chlamydia* Infection. Next, we used parabiosis surgery to examine whether these noncirculating memory cells were essential for immunity to secondary *Chlamydia* infection. *Cm*-immune (CD45.1) mice were surgically joined to congenic (CD45.2)-naïve mice and subsequently surgically separated after a period of shared circulation

(Fig. 2*A*). Successful parabiosis was confirmed by monitoring CD45.1- and CD45.2-expressing CD4 T cells in peripheral blood (Fig. 2 *C, Left*). Intravenous injection of CD90.2 antibody prior to tissue harvest confirmed that very few memory cells within the FRT are exposed to blood circulation in *Cm*-immune mice (Fig. 2*B*). As expected, the FRT of paired surgery control mice contained a 50:50 mix of IV-negative host and donor CD4 T cells expressing CD69 (Fig. 2*D*). Similarly, naïve parabionts had a mix of host and donor CD4 T cells (Fig. 2*D*), indicating efficient movement of donor immune memory cells into the FRT of naïve partners. In marked contrast, immune parabionts displayed a higher proportion of host CD4 T_{RM} within the FRT (Fig. 2 *C* and *D*). Thus, efficient chimerism occurs in the blood, but not the FRT, of parabiont-immune mice, consistent with previous reports (7). As expected (Fig. 1), CD4 T_{RM} in the FRT of immune mice displayed high surface levels

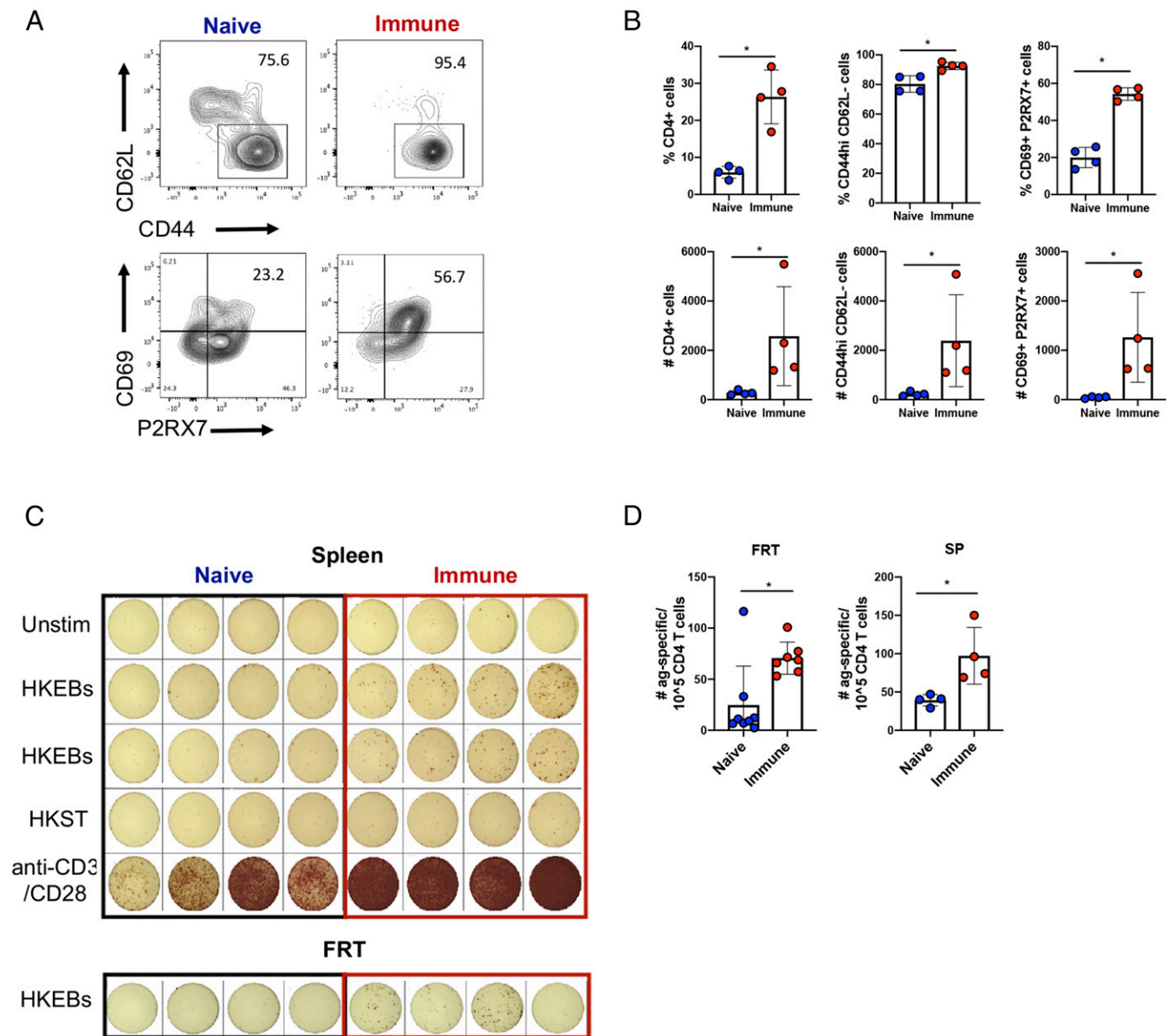


Fig. 1. *Chlamydia*-specific CD4 T_{RM} form in the FRT after I.Vag *Chlamydia* infection. Mice were infected I.Vag with 10⁵ IFU of *Cm* and euthanized after 50 to 65 d, weeks after the infection has cleared. (A) Flow plots of CD44^{hi} CD62L^{lo} CD4⁺ memory T cells and CD69⁺ P2RX7⁺ CD4⁺ T_{RM} in the FRT. (B) Quantification of percentage and number of CD4 T cells, CD4 memory T cells, and CD4 T_{RM}. (C) ELISPOT analysis of *Cm*-specific CD4 T cells in the spleen (Top) and FRT (Bottom) and (D) quantification. Significant differences were calculated using a Mann-Whitney *U* test. Data are means \pm SE; **P* < 0.5. *n* = 3 to 4 mice per group; data are representative of two experiments.

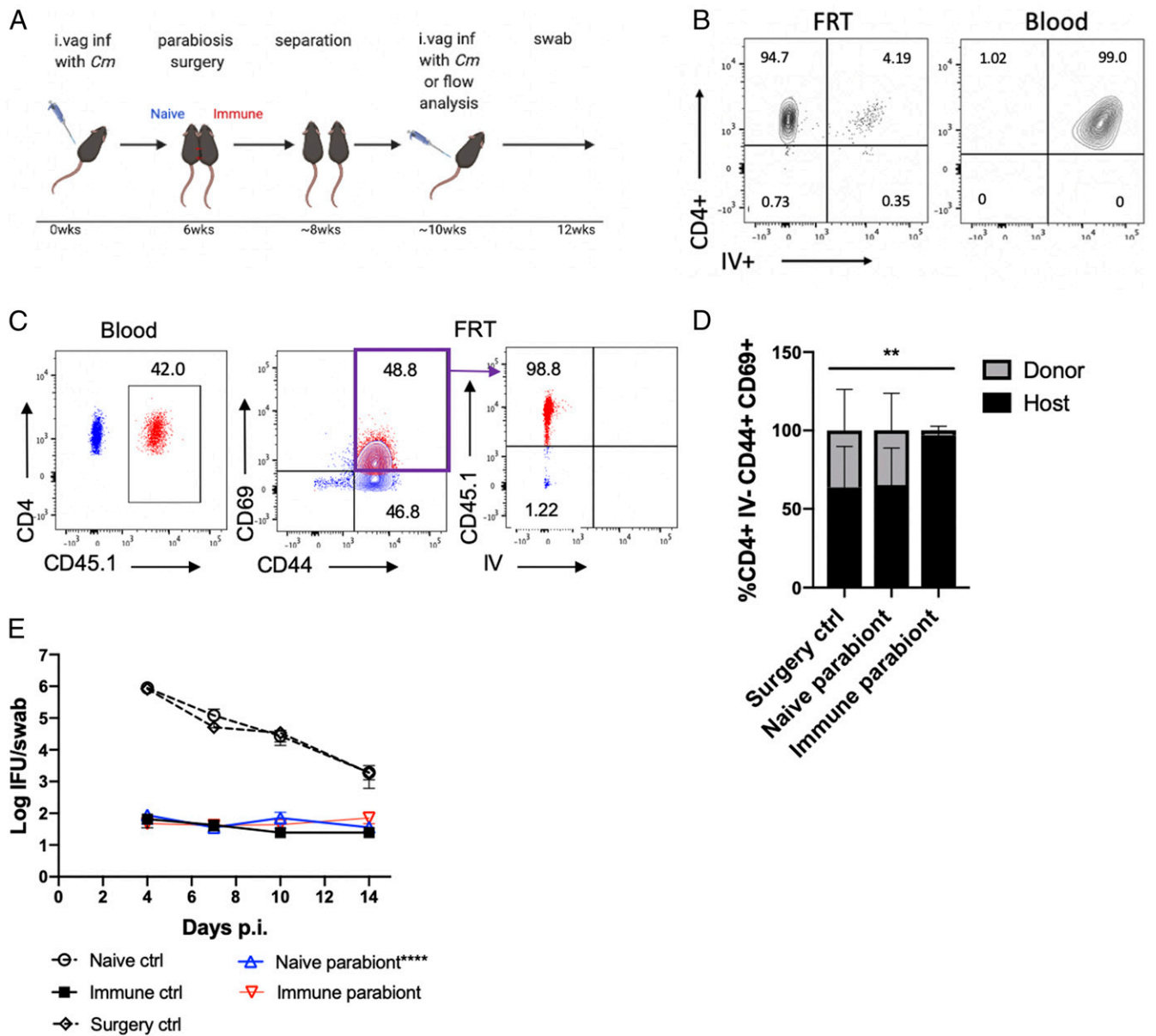


Fig. 2. Circulating memory is sufficient for protection against I.Vag *Chlamydia* challenge. Mice were infected I.Vag with 10^5 IFU of *Cm* and joined by parabiosis to naïve congenic, age-matched recipients after 6 wk. Two weeks later, mice were surgically separated and rested for another 2 wk. Mice were rechallenged with *Cm* or euthanized for flow analysis. (A) Schematic of experimental setup. (B) Example of intravenous labeling of lymphocytes in the blood. (C) Flow plots showing chimerism in the blood but not FRT of CD45.1+ immune parabionts. (Left) CD45.1-positive and -negative cells in the blood of parabionts. (Right) Example gating strategy for gating on CD69⁺ CD44^{hi} host and donor cells in parabiont FRTs. (D) Quantification of host and donor T_{RM} in parabiont FRTs. (E) Bacterial shedding of *Cm* from the reproductive tract of parabionts following secondary infection. Significant differences were calculated using a Mann–Whitney *U* test (D) and two-way ANOVA (E). Data are means \pm SE (D) or SEM (E); ***P* < 0.01, *****P* < 0.0001. *n* = 3 to 4 mice per group; data are representative of two experiments.

of CD44 and CD69 (Fig. 2 C, Right, and Fig. 2D). Intriguingly, circulating cells from the immune parabiont that entered the FRT of the naïve parabiont also expressed high levels of CD69 (Fig. 2 C and D).

This parabiosis approach allowed for the generation of mice with equivalent circulating memory but disparate FRT memory populations. After vaginal *Cm* challenge, all naïve and surgery control mice displayed high levels of bacterial shedding from the reproductive tract over 14 d (Fig. 2E). In marked contrast, immune parabionts successfully resisted secondary infection, demonstrating the presence of robust protective memory within the FRT (Fig. 2E; red triangles). Surprisingly, naïve parabionts also

displayed a robust protective response to secondary infection of the FRT, with almost no bacterial shedding (Fig. 2E; blue triangle). Thus, circulating memory transferred to naïve mice during parabiosis was fully sufficient to protect mice from *Chlamydia* infection of the FRT.

MLCs Are Not Required for Local Protection against *Chlamydia*.

Clusters of lymphocytes and APCs, termed MLCs, correlate with protection against herpes simplex virus infection of the lower reproductive tract (13). It has been hypothesized that similar clusters form after *Chlamydia* infection and are essential for secondary protection (12). Thus, MLC formation was measured in

immune and naïve parabiotic mice by staining tissue sections for CD4 T cells across the whole FRT (Fig. 3). MLCs (with a minimum radius of 75 μm) were enumerated in randomized sections by a blinded investigator (Fig. 3B). As expected, numerous MLCs were identified in the FRT of immune parabionts but were absent from the FRT of surgery control mice (Fig. 3C). Similarly, there were no MLCs detected in the FRT of naïve parabiotic mice (Fig. 3C) despite the fact that these mice resist vaginal infection with *Chlamydia* (Fig. 2E). Thus, transfer of immunity via parabiosis does not lead to MLC formation, and therefore MLCs are not essential for protection against local *Cm* infection.

Distal Mucosal Immunization with *Cm* Protects against Infection and Pathology in the FRT. IN exposure to live *Cm* protects mice against subsequent vaginal challenge; however, the degree of protection against bacterial load and pathology remains unclear (17). To compare protection in the FRT after local and distal immunization, mice were immunized intranasally or intravaginally with live *Cm* and challenged intravaginally. Distal immunization generated similar robust protection as observed with local immunization (Fig. 4A). To determine whether IN immunization with live *Cm* was capable of limiting upper reproductive tract (URT) pathology, uninfected, intranasally immunized and intravaginally infected mice, and mice that were only intravaginally infected were submitted for pathology scoring. All mice were euthanized for pathological analysis 30 d after I.Vag challenge. As expected, uninfected mice did not have high histopathological scores of their reproductive organs (Fig. 4B and C). Mice infected vaginally as a positive control developed severe composite lesion histopathology scores of the uterine horns and oviducts (Fig. 4B and C). In contrast, mice that were immunized intranasally before *Cm* challenge displayed significant protection against URT pathology (Fig. 4B and C). Thus, IN immunization is highly protective against local *Chlamydia*-induced infection and pathology of the FRT.

Local Protection against *Cm* Is Mediated by Circulating Memory CD4 T Cells. Since parabiosis experiments demonstrated that circulating immunity is sufficient for local protection (Fig. 2E), we

hypothesized that protection generated by distal immunization is also mediated by circulating immunity. To examine this possibility, we compared the generation of *Cm*-specific CD4 T cells in the spleen and FRT after IN or I.Vag immunization using ELISPOT. While *Cm*-specific CD4 T cells were detected in the spleen after either IN or I.Vag immunization, only I.Vag immunization generated *Cm*-specific CD4 T cell seeding of the FRT (Fig. 5A). Thus, IN immunization provides protection without generating FRT CD4 T_{RM} . To test whether circulating CD4 T cells provide local tissue protection after distal immunization, we depleted CD4+ lymphocytes from intranasally immunized mice (Fig. 5B) before I.Vag challenge with *Chlamydia* (Fig. 5C). CD4-depleted mice displayed elevated bacterial shedding from the FRT compared with isotype control mice, demonstrating that CD4 T cells provide circulating immunity in intranasally immunized mice (Fig. 5C). Increased local and systemic *Cm*-specific antibody responses were detected after IN immunization (SI Appendix, Fig. S1A), but passive transfer of immune serum failed to affect infection of the FRT (SI Appendix, Fig. S1C). Transfer of immune serum into the vaginal vault of mice on the same day as vaginal infection completely blocked *Cm* infection (SI Appendix, Fig. S1B), but this effect was rapidly lost if immune serum transfer was delayed by 1 d (SI Appendix, Fig. S1B). Thus, immediate encounter with mucosal antibody can prevent *Chlamydia* infection but has no effect after infection has commenced. These data show that circulating CD4 T cells generated by distal mucosal immunization are required to control *Chlamydia* infection locally in the FRT.

Discussion

Tissue-resident memory cells have been shown to play a vital role in protection in models of genital infection (7, 9, 11, 13, 14), leading to the generalization that T_{RM} protect barrier tissues. In marked contrast, our data demonstrate robust pathogen control within the FRT that is independent of T_{RM} . While efficient generation of T_{RM} and MLCs occurs in mice that resolve primary *Chlamydia* infection, this is not a requirement for protection against local mucosal infection. Using two different experimental models (parabiosis and IN immunization), we find solid protection

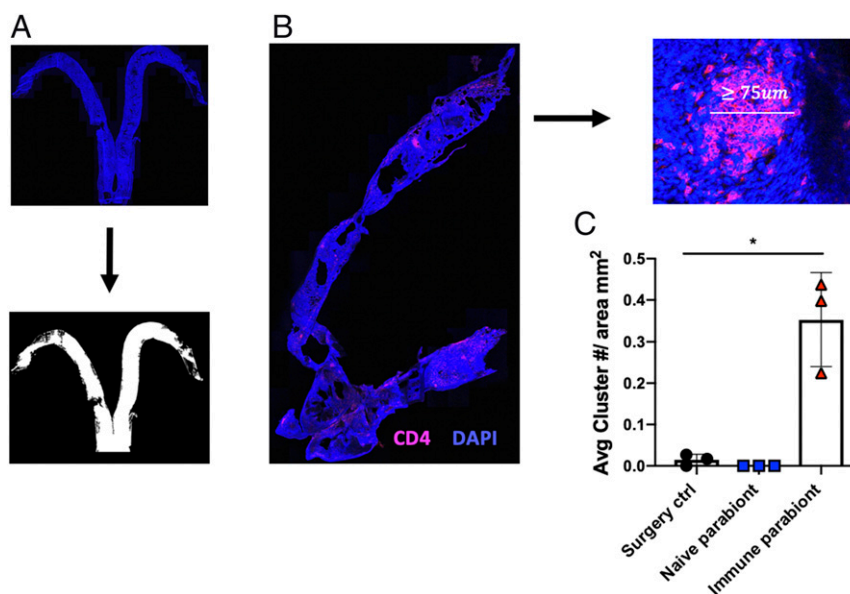


Fig. 3. MLCs form in the FRT after *Cm* infection but are not required for protection. FRTs from parabionts were frozen, sectioned, and stained with DAPI and Pe Texas Red for CD4+ cells. (A) Areas of tissue sections were masked based on DAPI staining and calculated using ImageJ. (B) Clusters of CD4 T cells were counted by eye and divided by the area of DAPI staining. (C) Clusters per area averaged per mouse. Significant differences were calculated using a Kruskal–Wallis test and two-way ANOVA (C). Data are means \pm SE; * $P < 0.5$. $n = 3$ mice per group; data are representative of one experiment.

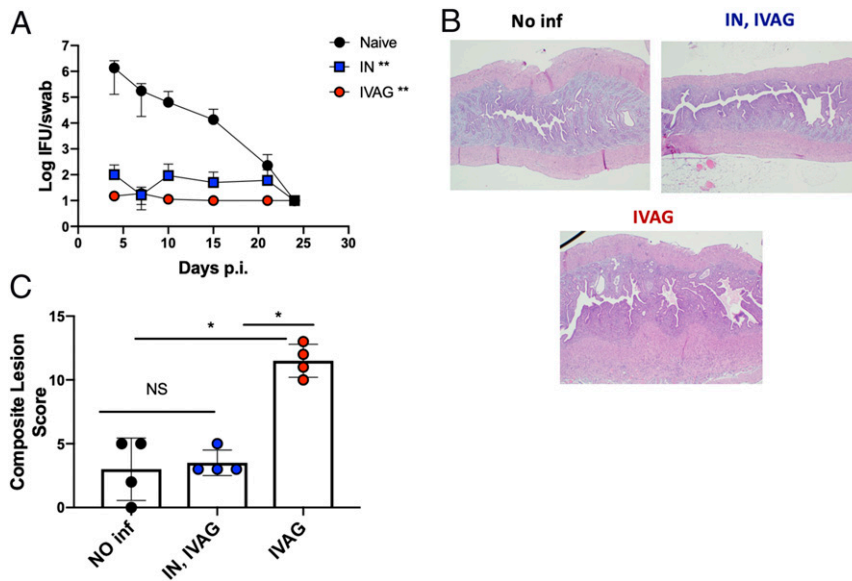


Fig. 4. Protection against FRT infection and pathology after IN immunization with *Cm*. Mice were intranasally immunized with 10^5 IFU of *Cm* and then challenged intravaginally 47 d later. (A) Bacterial shedding measured by vaginal swabs. Significant differences were calculated using a two-way ANOVA. To determine protection against FRT pathology, mice were immunized intranasally with 10^5 IFU of *Cm* or left unimmunized and challenged 42 d later with the same dose intravaginally. A total of 30 d after the secondary challenge, mice were analyzed for FRT pathology. Uninfected mice were included as controls. (B) Example images of H&E staining of mouse uterine tissue at 20 \times magnification. (C) Composite lesion pathology scores of uterine and oviduct tissues. Significance between groups was calculated using a Mann–Whitney *U* test. Data represent one experiment with $n = 4$ mice per group. Data are means \pm SE; * $P < 0.5$, ** $P < 0.01$. H&E, hematoxylin and eosin; NS, not significant; p.i., postinfection.

of the FRT in the absence of local T_{RM} or MLCs. Instead, local protection is provided by circulating memory CD4 T cell responses that are induced elsewhere. This finding is important for two reasons. First, it validates the historical and ongoing examination of immune memory within the peripheral blood of patients with current or previous genital tract infection in the search for

correlates of protection. Second, it suggests that vaccine development against vaginal infection may not necessarily require induction of local tissue memory responses and traditional parenteral immunization could be sufficient.

Although our data show that *Chlamydia* infection of the FRT induces strong circulating memory responses, it is also clear that

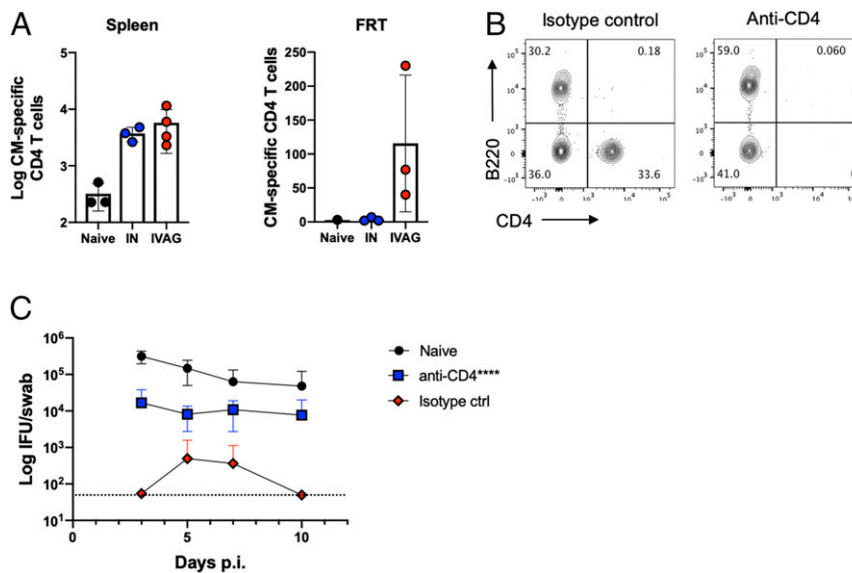


Fig. 5. Protection after IN immunization is dependent on CD4 T cells. Mice were intranasally or intravaginally immunized with 10^5 IFU of *Cm*, and CD4 T cells from FRTs and spleens were analyzed 56 d later by ELISPOT for IFN- γ secretion after *Chlamydia* stimulation. (A) Number of *Cm*-specific CD4⁺ T cells in the spleen and FRT of mice from all groups. Significance between groups was calculated using a Mann–Whitney *U* test. To test the requirement of circulating CD4 T cells for controlling secondary infection, mice were immunized intranasally with 10^4 IFU of *Cm* and rechallenged I.Vag with 10^6 IFU 93 d later. Mice were treated with anti-CD4 antibody or isotype control antibody beginning 4 d prior to secondary challenge and through day 18 postinfection. (B) Example flow plots of B220⁺ and CD4⁺ cells in the blood of anti-CD4- and isotype control-treated mice 5 d postinfection. (C) Bacterial shedding curve of secondary infection. Significant differences between groups were calculated using a two-way ANOVA. Data are means \pm SE (C); **** $P < 0.0001$. p.i., postinfection.

natural *Chlamydia* exposure generates a strong T_{RM} response and the formation of MLCs. While these local memory responses are not essential for protection, it seems likely that they participate in secondary immune responses. Indeed, the presence of local T_{RM} may be more critical in viral infection models due to the faster replication rate of some viruses (herpes simplex virus, 4 to 12 h) (18) compared with *Chlamydia* (48 h) (19). We suggest that the nature of the pathogen might dictate the need for this specialized layer of poised immunity at barrier tissues rather than there being a general requirement for T_{RM} in barrier defense. The longevity of different memory populations is not directly addressed by our study but may be a critical variable. While circulating memory responses can decline over time, our previous study demonstrated a robust elevated population of *Chlamydia*-specific CD4 T cells in secondary lymphoid organs 352 d after primary infection (5). Future studies will be needed to examine whether antigen or bacterial persistence affects the maintenance of this memory pool.

Circulating immunity induced after IN immunization consisted of both antigen-specific CD4 T cells and IgG antibodies, and recent studies point to an important role for antibody in *Chlamydia* protection (20, 21). Local secretion of *Cm*-specific IgG was detected in the FRT after IN immunization, and the injection of serum into the vaginal vault efficiently blocked infection. These data support the idea that antibody is an important component of barrier defense against reproductive tract pathogens. However, depletion of CD4 T cells eliminated almost all of the protective effect of circulating memory, suggesting that circulating T cells are the critical limiting factor in *Chlamydia* immunity. We propose a model in which antibodies secreted lumenally may sometimes be sufficient to efficiently block *Chlamydia* attachment or entry into the vaginal epithelium and eliminate infection.

However, if this initial barrier defense fails, recruitment of circulating CD4 T cells will be required to control the established infection within the FRT. It is currently unclear whether the antibody secreted in the FRT mucosa after IN immunization is derived from serum antibody or from plasma cells within the FRT. This should be a focus of future studies since it may be critical for vaccine development. While our data demonstrate a CD4-dependent mechanism of *Chlamydia* protection, the precise mechanism of CD4-mediated immunity within the FRT is an enigma. While IFN- γ -mediated induction of cell intrinsic defense mechanisms (22, 23) or cytotoxic killing of infected epithelial (24) seem likely possibilities, this will also require more detailed analysis of CD4 effector function within the FRT.

In summary, our data show a surprising capacity of circulating memory CD4 T cells to efficiently protect against one of the most common human pathogens to infect mucosal surfaces. This capacity to disconnect protection from T_{RM} and MLC formation is encouraging since it suggests a roadmap to successful vaccination without the need for encouraging local tissue-specific adaptations that may be more difficult to induce.

Data Availability. All study data are included in the article and/or *SI Appendix*.

ACKNOWLEDGMENTS. We thank the UC Davis Veterinary Medicine Advanced Imaging Facility and Ingrid Brust-Mascher for assistance with imaging tissues. We also thank the Comparative Pathology Laboratory at UC Davis for conducting histopathological analyses of tissues in this study. This work was funded by the National Institute of Allergy and Infectious Diseases (R01AI103433, R01AI139047, R01AI139410, and T32AI060555) and the Sims Immunology Fellowship.

1. A. A. Itano, M. K. Jenkins, Antigen presentation to naive CD4 T cells in the lymph node. *Nat. Immunol.* **4**, 733–739 (2003).
2. J. Zhu, W. E. Paul, Heterogeneity and plasticity of T helper cells. *Cell Res.* **20**, 4–12 (2010).
3. D. Masopust, J. M. Schenkel, The integration of T cell migration, differentiation and function. *Nat. Rev. Immunol.* **13**, 309–320 (2013).
4. R. L. Gieseck III, M. S. Wilson, T. A. Wynn, Type 2 immunity in tissue repair and fibrosis. *Nat. Rev. Immunol.* **18**, 62–76 (2018).
5. L.-X. Li, S. J. McSorley, B cells enhance antigen-specific CD4 T cell priming and prevent bacteria dissemination following *Chlamydia muridarum* genital tract infection. *PLoS Pathog.* **9**, e1003707 (2013).
6. J. M. Benoun *et al.*, Optimal protection against *Salmonella* infection requires non-circulating memory. *Proc. Natl. Acad. Sci. U.S.A.* **115**, 10416–10421 (2018).
7. L. K. Beura *et al.*, CD4⁺ resident memory T cells dominate immunosurveillance and orchestrate local recall responses. *J. Exp. Med.* **216**, 1214–1229 (2019).
8. J. M. Schenkel *et al.*, T cell memory. Resident memory CD8 T cells trigger protective innate and adaptive immune responses. *Science* **346**, 98–101 (2014).
9. J. E. Oh *et al.*, Migrant memory B cells secrete luminal antibody in the vagina. *Nature* **571**, 122–126 (2019).
10. Y. Nakanishi, B. Lu, C. Gerard, A. Iwasaki, CD8(+) T lymphocyte mobilization to virus-infected tissue requires CD4(+) T-cell help. *Nature* **462**, 510–513 (2009).
11. J. M. Schenkel, K. A. Fraser, V. Vezy, D. Masopust, Sensing and alarm function of resident memory CD8⁺ T cells. *Nat. Immunol.* **14**, 509–513 (2013).
12. R. M. Johnson, R. C. Brunham, Tissue-resident T cells as the central paradigm of *Chlamydia* immunity. *Infect. Immun.* **84**, 868–873 (2016).
13. N. Iijima, A. Iwasaki, T cell memory. A local macrophage chemokine network sustains protective tissue-resident memory CD4 T cells. *Science* **346**, 93–98 (2014).
14. G. Stary *et al.*, VACCINES. A mucosal vaccine against *Chlamydia trachomatis* generates two waves of protective memory T cells. *Science* **348**, aaa8205 (2015).
15. H. Shin, A. Iwasaki, Generating protective immunity against genital herpes. *Trends Immunol.* **34**, 487–494 (2013).
16. H. Shin, A. Iwasaki, A vaccine strategy that protects against genital herpes by establishing local memory T cells. *Nature* **491**, 463–467 (2012).
17. S. Pal, E. M. Peterson, L. M. de la Maza, Intranasal immunization induces long-term protection in mice against a *Chlamydia trachomatis* genital challenge. *Infect. Immun.* **64**, 5341–5348 (1996).
18. D. L. Wiedbrauk, “Herpes simplex virus” in *Molecular Diagnostics*, W. W. Grody, R. M. Nakamura, C. M. Strom, F. L. Kiechle, Eds. (Academic Press, San Diego, 2010), chap. 37, pp. 453–460.
19. R. C. Brunham, J. Rey-Ladino, Immunology of *Chlamydia* infection: Implications for a *Chlamydia trachomatis* vaccine. *Nat. Rev. Immunol.* **5**, 149–161 (2005).
20. L.-X. Li, S. J. McSorley, A re-evaluation of the role of B cells in protective immunity to *Chlamydia* infection. *Immunol. Lett.* **164**, 88–93 (2015).
21. P. A. Malaviarachi, M. A. B. Mercado, S. J. McSorley, L. X. Li, Antibody, but not B-cell-dependent antigen presentation, plays an essential role in preventing *Chlamydia* systemic dissemination in mice. *Eur. J. Immunol.* **50**, 676–684 (2020).
22. J. A. Ibana *et al.*, *Chlamydia trachomatis*-infected cells and uninfected-bystander cells exhibit diametrically opposed responses to interferon gamma. *Sci. Rep.* **8**, 8476 (2018).
23. D. E. Nelson *et al.*, *Chlamydia* IFN- γ immune evasion is linked to host infection tropism. *Proc. Natl. Acad. Sci. U.S.A.* **102**, 10658–10663 (2005).
24. K. Jayarapu, M. Kerr, S. Ofner, R. M. Johnson, *Chlamydia*-specific CD4 T cell clones control *Chlamydia muridarum* replication in epithelial cells by nitric oxide-dependent and -independent mechanisms. *J. Immunol.* **185**, 6911–6920 (2010).